THE BELL SYSTEM TECHNICAL JOURNAL
Vol. 56, No. 8, October 1977
Printed in U.S.A.

Some Experiments in Adaptive and Predictive Hadamard Transform Coding of Pictures

By A. N. NETRAVALI, B. PRASADA, and F. W. MOUNTS

(Manuscript received April 15, 1977)

This paper describes some experiments in adaptive and predictive Hadamard transform coding of still pictures using a small transform block (2 × 2 × 2). Predictive coding of the transform coefficients is discussed using certain combinations of coefficients of the present as well as previously transmitted blocks as predictors. Two separate adaptive quantization techniques are considered. The first technique relates to PCM quantization, in which a uniform PCM quantizer with a different number of quantization levels is used, depending upon the spatial activity within the block. The second technique alters the quantizer of a predictive transform coder based on a weighted sum of already transmitted coefficients of the present and previous blocks. Finally, we give a comparison of three coding techniques: (i) adaptive predictive transform coding, (ii) nonadaptive transform coding, and for comparison, (iii) nonadaptive predictive coding in the picture element domain using a two-dimensional prediction.

I. INTRODUCTION

In a recent paper[1] we considered Hadamard transform coding of still pictures using a small three-dimensional block (a 2 × 2 × 2 array of picture elements). There we described the design of optimum quantizers for the Hadamard transform coefficients based on psychovisual criteria in the transform domain. Starting with subjective tests to evaluate the visibility of quantization noise, we then developed a design procedure to minimize the "mean-square subjective distortion" (MSSD) due to quantization noise. We compared the performance of the resulting quantizers with the widely used Max-type[2] quantizers (i.e., quantizers which minimize the mean-square quantization error) and demonstrated our quantizers to be better in terms of picture quality and entropy of the quantizer output, for a given number of levels.

The present paper, which consists of three parts, extends the previous

work by considering techniques for adaptive and predictive coding of the transform coefficients, based on both statistical and psychovisual criteria. In the first part, we develop prediction algorithms for predictive coding of the coefficients. Although the small block size that we use ensures that the quantization noise can be placed in those parts of the picture where it is least visible, thereby permitting coarser quantization and thus achieving a higher coding efficiency, it does not exploit the statistical correlation between adjacent blocks. To overcome this, we consider predictive coding for the coefficients. We predict the value of a coefficient using a linear combination of already-transmitted values of other coefficients of both the present and the previous block. The prediction error is then quantized and transmitted. A reverse operation is performed at the receiver to reconstruct the picture elements. Our predictors are not limited to small block sizes. We show how they can be extended to larger spatial blocks as well as to spatiotemporal blocks.

The second part of this paper is concerned with two separate techniques for adaptive quantization, one useful in PCM quantization and the other in predictive quantization of the coefficients. These adaptive quantizers change to match the fidelity requirements of a viewer in different parts of the picture, as measured by subjective tests. We illustrate our methodology only for the coding of the first Hadamard coefficient. In PCM quantization, we use coefficients within a block representing a measure of spatial detail, to determine when to change the number of levels of the quantizer. Based on a theoretical analysis, we obtain a formula to change the number of quantizer levels and demonstrate the usefulness of this formula on a hardware system. In predictive quantization, the quantizers are switched on the basis of a weighted sum of the coefficients of the present and previous blocks. In areas of low spatial detail, a fine quantizer optimized for that area is used, whereas in areas of high spatial detail, a coarse quantizer is used which is optimized for such an area. The advantage of adapting the quantizer is evaluated by measuring the entropy for a given picture quality.

The third part of the paper deals with some comparisons between the techniques discussed in the first two parts and in our previous paper[1]. These comparisons are based on the picture quality versus entropy tradeoffs. They show that adaptive-predictive transform coding requires about 1.84 bits/pel for an excellent picture quality; and this represents, for the same picture quality, a decrease of almost 1.3 bits/pel over the bit rate obtainable by two-dimensional predictive coding in the picture element (pel) domain.

1.2 Relationship with some previous work

The combining of transform coding with predictive coding has been

discussed by many authors. Reudink[3] investigated simple DPCM coding of Hadamard transform coefficients which are obtained from a transform of 4, 8, or 16 pels along a scan line of video. Habibi[4] generalized the combining of transform and predictive coding. He considered several different transforms using one-dimensional blocks or small two-dimensional blocks and found that such a hybrid coding system performed better, in terms of signal-to-noise ratio for a given bit rate, than either the transform coding or the predictive coding system separately. Ishii[5] has considered a similar coding scheme using Hadamard transform coding, whereas Heller[6] and Roese et al.[7] have extended this concept to interframe coding.

Our contribution here is twofold. First, we develop methods for prediction that use coefficients from the present as well as previous blocks. Second, we develop a technique to quantize coefficients taking into account subjective effects of the quantization noise.

Adaptive coding of transform coefficients has been discussed by many authors.[8] Simple techniques of threshold sampling, which transmit only those coefficients whose magnitudes exceed a certain threshold, have been in existence for some time. Tasto and Wintz[9] have used local statistical properties of pictures to divide the picture into a number of segments and have chosen the coding strategy suited for each subpicture. Their division of pictures does depend on spatial activity, although not explicitly. It should be noted that their "best" quantizers were from those encountered in their trial-and-error procedure. Gimlett[10] has proposed a definition of an "activity index" using a weighted sum of absolute values of the transform coefficients and assigned more bits for coding those subpictures having a higher "activity index". This does not take advantage of the observer's reduced sensitivity for reproducing areas of higher activity.

Our adaptive quantization techniques divide the picture on the basis of subjective noise visibility and then design the quantizer for each segment. This is done using the data from the subjective tests in which noise visibility is related to certain measures of spatial detail.

II. PREDICTORS FOR TRANSFORM COEFFICIENTS

The objective of this section is to show that, for predictive coding of the transform coefficients, predictions better than the corresponding coefficients from the previous block can be made. In general, a predictor can utilize the information contained in the corresponding coefficient as well as other coefficients of the previous block. It can also utilize information contained in the other coefficients of the same block that may be available to the receiver when reconstructing the coefficient which is being differentially encoded.

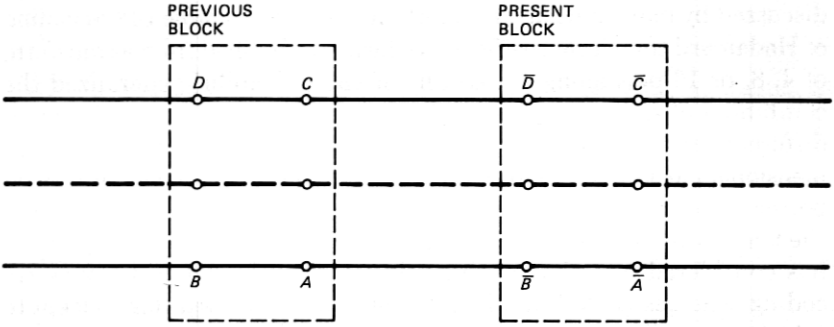

Fig. 1—Pel locations of two successive Hadamard transform blocks.

To illustrate the technique, we take a specific example of a 2×2 block of pels and develop a predictor for H_1, the first transform coefficient. The configuration of the block is shown in Fig. 1, where A is the current pel, B is the previous pel in the same line, C is the pel corresponding to A in the previous line in the same field, and D is the previous element with respect to C. After Hadamard transformation, the four coefficients are defined as follows:

$$\begin{aligned} H_1 &= A + B + C + D \\ H_2 &= A + B - C - D \\ H_3 &= A - B - C + D \\ H_4 &= A - B + C - D \end{aligned} \tag{1}$$

Now consider two horizontally consecutive blocks (as in Fig. 1), one having pels A, B, C, D giving rise to coefficients H_1, H_2, H_3, H_4; and the other having pels $\overline{A}, \overline{B}, \overline{C}, \overline{D}$ giving rise to coefficients $\overline{H}_1, \overline{H}_2, \overline{H}_3, \overline{H}_4$. Then the prediction for $\overline{H}_1$ is taken to be

$$(H_{1Q} + H_{4Q} + \overline{H}_{4Q}) \tag{2}$$

where subscript Q denotes the quantized values available both at the transmitter and the receiver. The prediction error is evaluated, quantized and transmitted.

The prediction error in the absence of quantization will be

$$\begin{aligned} \Delta\hat{H}_1 &= \overline{H}_1 - H_1 - H_4 - \overline{H}_4 \\ &= (\overline{D} - C) + (\overline{B} - \mathrm{A}) + (\overline{D} - \mathrm{C}) + (\overline{B} - A) \end{aligned} \tag{3}$$

From Fig. 1, $(\overline{D} - C)$ and $(\overline{B} - A)$ are the element differences and are, in general, small. Thus, the problem of transmitting H_1 is converted to the problem of transmitting a sum of certain element differences. The prediction error using the previous block H_1 as the prediction of $\overline{H}_1$ is

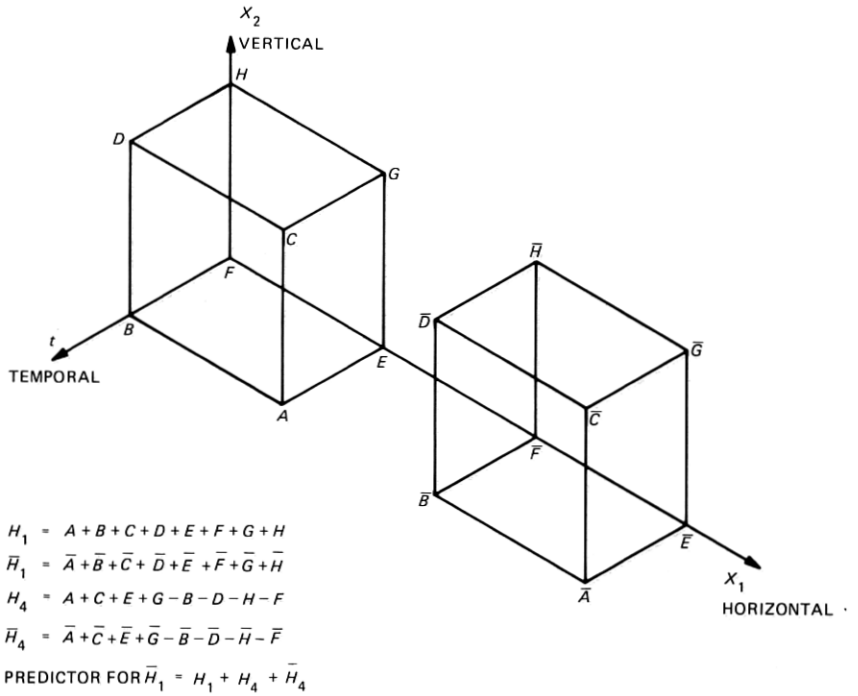

Fig. 2—Predictor for $\overline{H}_1$ of a spatiotemporal transform block.

given by

$$\Delta H_1 = \overline{H}_1 - H_1$$
$$= (\overline{D} - C) + (\overline{B} - A) + (\overline{C} - D) + (\overline{A} - B) \qquad (4)$$

Comparing the prediction errors [eqs. (3) and (4)], we see that the first two terms of the right-hand side are identical. However, the next two terms in eq. (4) will in general have higher values due to larger spatial separation, and therefore the predictor shown in eq. (2) will have a lower average error.

The example described above can be extended to more general cases than a spatial block of 2×2. Thus, better prediction of $\overline{H}_1$ is possible in the case of spatiotemporal blocks as well as larger spatial blocks. As an illustration, we show in Fig. 2 a case with a $2 \times 2 \times 2$ "spatiotemporal" block. The definition of the predictor is shown in the same figure. Notice that the prediction error can again be written as a summation of certain spatially adjacent element differences and this reduces the entropy of the prediction error.

The above procedure can be used for constructing better predictors for other transform coefficients. As an example for the blocks in Fig. 1,

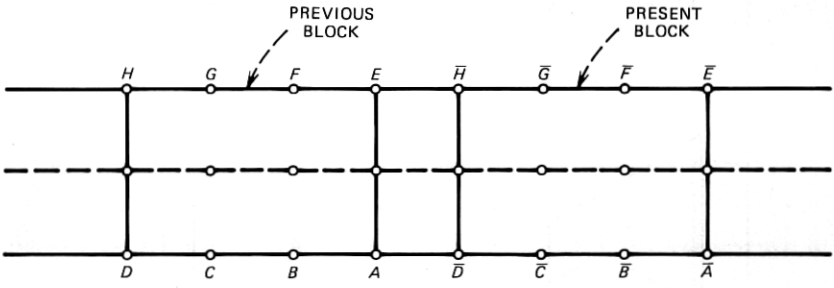

Fig. 3—Pel locations of two successive large transform blocks.

the predictor for $\overline{H}_2$ is taken to be

$$(H_2 + H_3 + \overline{H}_3) \tag{5}$$

It is easy to see that the prediction error is given by

$$2\{\overline{B} + C - (A + \overline{D})\} \tag{6}$$

which is two times H_3 of the intermediate block with pels $\{\overline{B}, A, \overline{D}, C\}$. Since H_3 generally has very small value, the prediction error will again have lower entropy as compared to the entropy of $(\overline{H}_2 - H_2)$. We note in passing that, instead of using a horizontally adjacent block as above, coefficients from the vertically adjacent block can also be used to construct predictors (e.g., the prediction for $\overline{H}_4$ can be $(H_4^V + H_3^V + \overline{H}_3)$, where superscript V denotes coefficients from the vertically adjacent block).

As an extension of our predictor to larger blocks, consider a block of 8 pels as shown in Fig. 3. Hadamard transformation of the pels from "previous block" gives us

$$\begin{bmatrix} H_1 \\ H_2 \\ H_3 \\ H_4 \\ H_5 \\ H_6 \\ H_7 \\ H_8 \end{bmatrix} = \begin{vmatrix} 1 & 1 & 1 & 1 & 1 & 1 & 1 & 1 \\ 1 & 1 & 1 & 1 & -1 & -1 & -1 & -1 \\ 1 & 1 & -1 & -1 & -1 & -1 & 1 & 1 \\ 1 & 1 & -1 & -1 & 1 & 1 & -1 & -1 \\ 1 & -1 & -1 & 1 & 1 & -1 & -1 & 1 \\ 1 & -1 & -1 & 1 & -1 & 1 & 1 & -1 \\ 1 & -1 & 1 & -1 & -1 & 1 & -1 & 1 \\ 1 & -1 & 1 & -1 & 1 & -1 & 1 & -1 \end{vmatrix} \begin{bmatrix} A \\ B \\ C \\ D \\ E \\ F \\ G \\ H \end{bmatrix} \tag{7}$$

Hadamard transformation of the pels from the "present block" which generates $\overline{H}_1, \ldots, \overline{H}_8$ are similarly defined. The prediction error by using H_1 as a prediction of $\overline{H}_1$ is given by

$$\begin{aligned} \overline{H}_1 - H_1 = [&(\overline{D} - A) + (\overline{C} - B) + (\overline{H} - E) + (\overline{G} - F) \\ &+ (\overline{B} - C) + (\overline{A} - D) + (\overline{F} - G) + (\overline{E} - H)] \end{aligned} \tag{8}$$

We note that the last four terms of the right-hand side are often larger because of the wider separation of picture elements. A better predictor

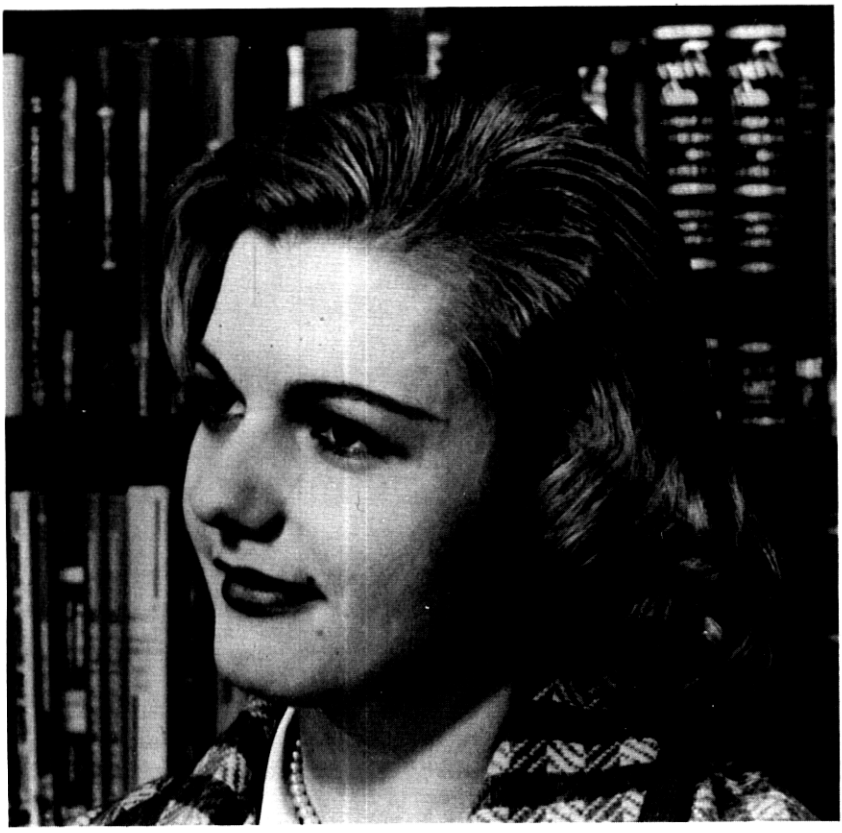

Fig. 4—Original picture used for subjective tests.

for $\overline{H}_1$ is taken to be $H_1 + H_4 + \overline{H}_4$ and then the prediction error would be

$$= [(\overline{D} - A) + (\overline{C} - B) + (\overline{H} - E) + (\overline{G} - F) + (\overline{D} - A) + (\overline{C} - B) + (\overline{H} - E) + (\overline{G} - F)] \quad (9)$$

The first four terms of eqs. (8) and (9) are equal; but comparing the last four terms, we see that in general the right-hand side of eq. (9) would be smaller than that of eq. (8).

We evaluated the performance of the new prediction scheme by hardware simulation using a $2 \times 2 \times 2$ block. We considered a still picture; and, therefore, except for frame-to-frame noise, this is equivalent to considering a 2×2 block. The picture entitled "Library Girl" shown in Fig. 4 was used for all the experiments discussed in this paper. We calculated the entropy of the unquantized prediction error for both predictors. The entropy of prediction error of eq. (3) was 4.99 bits/block,

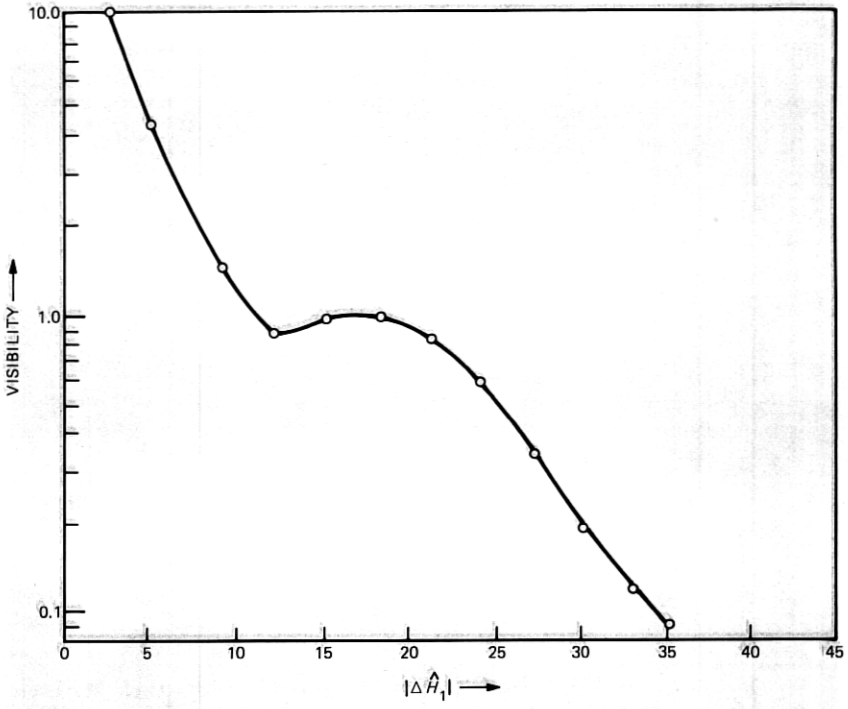

Fig. 5—Visibility function for noise in H_1. Prediction error $|\Delta \hat{H}_1|$ is used as a control variable.

and of eq. (4) was 6.35 bits/block, clearly showing that the new predictor is better for the picture used. Quantizers were then designed for each of these predictors. They were optimized by performing subjective experiments to measure the visibility of quantization noise as a function of the unquantized prediction error; and then, following a procedure analogous to that in Ref. 1, the mean-square subjective distortion due to quantization noise was minimized. We note that the prediction error $\Delta \hat{H}_1$ with respect to which the noise visibility is determined in these experiments is a better choice than ΔH_1 since $\Delta \hat{H}_1$ is the sum of element differences spatially closer to block $\{\overline{A}, \overline{B}, \overline{C}, \overline{D}, \overline{E}, \overline{F}, \overline{G}, \overline{H}\}$, where the quantization error appears. This provides a better spatial masking of the quantization noise.

The visibility function* $f_{H_1}(\cdot)$ for noise in H_1 as a function of $\Delta \hat{H}_1$ is shown in Fig. 5. Quantizers were obtained for a different number of quantization levels (N), and their performance was observed by the authors. For $N = 21$, a fairly good picture was obtained with an entropy of 3.13 bits/block. There was a noticeable (not objectionable) noise

* The method of obtaining visibility function is described in Ref. 1.

pattern with some structure in the gray regions. For $N = 23$, very good picture quality was obtained. A noise pattern was slightly visible in the gray regions of the picture, and the entropy was 3.17 bits/block. For $N = 25$, a near perfect picture was obtained with a very slight amount of noise in the gray regions of the picture. The entropy was 3.19 bits/block.

During these evaluations, the other coefficients H_2, H_3 and H_4 were unquantized. Even though the picture was stationary, the experiment was done in real time, so that the effects of camera noise which changes from frame to frame were included.

It is interesting to compare these observations with results[1] obtained using H_1 as the predictor for $\overline{H}_1$. In that case, a near perfect picture was obtained with $N = 36$ and an entropy of 4.25 bits/block. This shows that the new predictor gave about 25 percent lower entropy than the previous block coefficient predictor.

III. ADAPTIVE QUANTIZATION OF THE FIRST COEFFICIENT

In this part we discuss two separate techniques for the adaptive quantization of the first transform coefficient H_1. The first technique is applicable to PCM quantization, and the second to DPCM quantization of the coefficients.

The general approach is to identify measures of spatial luminance activity in terms of certain transform coefficients and then to obtain relations between noise visibility and these measures by subjective experiments. The visibility function is used for the categorization of blocks into subpictures of approximately equal visibility for a given quantity of noise. Separate quantizers are used for each category. We will now describe the application of this general approach for the quantization of H_1.

3.1 Adaptive PCM quantization of H_1

In general, a picture may be categorized into several regions depending on spatial detail. H_1 can be specified with different accuracy in each of these regions without degrading the picture quality as seen by a human viewer. The magnitude of either H_2 or H_4 or both is large in the busy regions of the picture and, hence, is taken as an indication of picture busyness. Since H_2 and H_4 are available to the receiver prior to decoding of H_1, there is no need to transmit information regarding the adaptation of coding of H_1 explicitly to the receiver.

3.1.1 Design of adaptive PCM Quantizer for H_1 as a function of $|H_2|$, $|H_4|$

Let

$$x = \max(|H_2|, |H_4|)$$

$f(x)$ = visibility function for noise in H_1 obtained as a function of x

$p(x)$ = probability density of x, measured for picture of Fig. 4.

We carry out our derivation for a uniform quantizer with "ℓ_1" levels used for quantizing H_1 from all blocks where $0 \leq x \leq x_1$, x_1 being a positive number, and "ℓ_2" levels used for all other cases. Assuming that the quantization noise is proportional to $1/(\ell_i)^\gamma$, $i = 1, 2$, for a positive constant γ, we can express the visible distortion (D) due to the quantization noise as†

$$D = \frac{1}{\ell_1^\gamma} \int_0^{x_1} f(x)\, dx + \frac{1}{\ell_2^\gamma} \int_{x_1}^{\infty} f(x)\, dx \tag{10}$$

Assuming no variable-length coding, the average number of bits required for such quantization is†

$$B = \log \ell_1 \int_0^{x_1} p(x)\, dx + \log \ell_2 \int_{x_1}^{\infty} p(x)\, dx \tag{11}$$

Using calculus of variations, we solve the problem of minimizing D, for a given B, with respect to ℓ_1, ℓ_2, and x_1. It is seen that the optimum ℓ_1 and ℓ_2, defined as ℓ_1^*, ℓ_2^*, are given by

$$\ell_1^* \propto \left(\frac{\gamma \int_0^{x_1} f(x)dx}{\int_0^{x_1} p(x)dx} \right)^{1/\gamma} \tag{12a}$$

$$\ell_2^* \propto \left(\frac{\gamma \int_{x_1}^{\infty} f(x)dx}{\int_{x_1}^{\infty} p(x)dx} \right)^{1/\gamma} \tag{12b}$$

Also the optimum x_1^* is given by

$$\frac{f(x_1^*)}{p(x_1^*)} \propto \frac{\log (\ell_2^*/\ell_1^*)}{(\ell_1^*)^{-\gamma} - (\ell_2^*)^{-\gamma}} \qquad (\ell_1^* \neq \ell_2^*) \tag{12c}$$

As shown in the next section, we simulated a system with adaptive quantization to check the above equations.

3.1.2 Experimental investigation and results

An experiment was performed to obtain a value of γ and to verify the result of Section 3.1.1. First, the visibility function was obtained by subjective testing. Figure 6 shows the visibility function $f(x)$ obtained with x as the control function.

† Except for a proportionality constant.

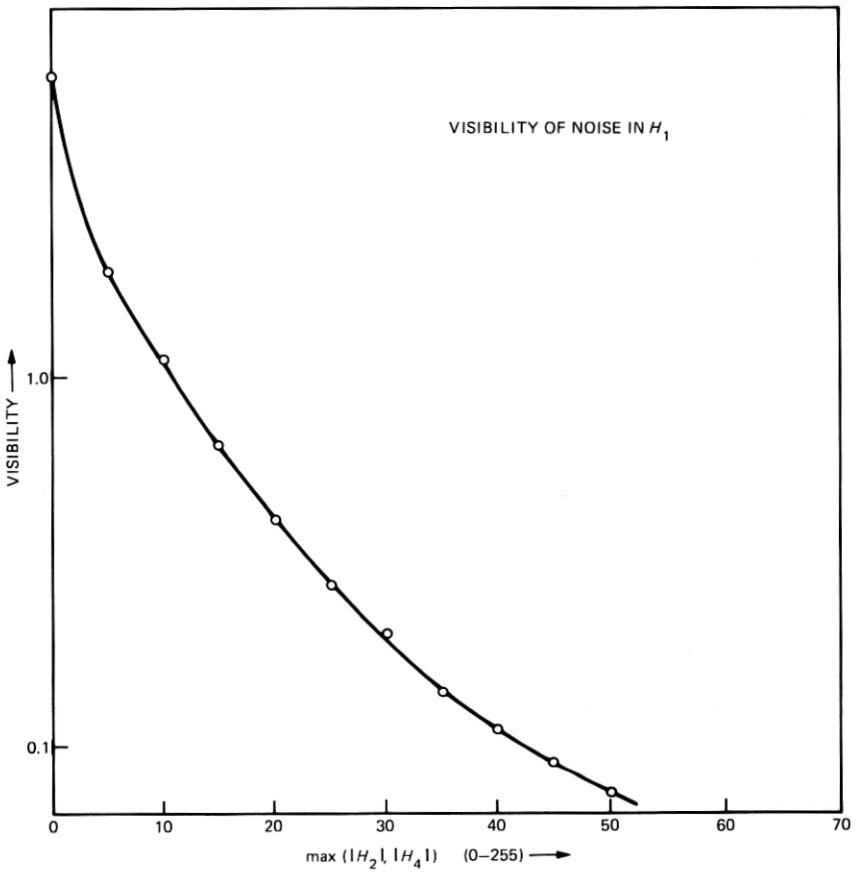

Fig. 6—Visibility function for noise in H_1. Max ($|H_2|$,$|H_4|$) is used as a control variable.

In the experiment, two quantizers, Q_A and Q_B, were used to quantize H_1. For a block, the function $x = \max(|H_2|,|H_4|)$ was determined† and the value compared with a threshold to decide whether quantizer Q_A or Q_B should be used. The block diagram of the experimental setup is shown in Fig. 7. Condition I refers to nonadaptive quantization of H_1 by a uniform quantizer. We considered two cases: for case 1 the uniform quantizer uses 128 levels, and for case 2, 64 levels. Condition II pertains to quantization of H_1 by either quantizer Q_A (for $x \leq T$) or quantizer Q_B (for $x > T$). In an A–B test, two subjects compared pictures corresponding to conditions I and II and adjusted the threshold T to the smallest value at which the pictures appeared to be of the same quality.

† Effect of quantization of H_2 and H_4 was neglected.

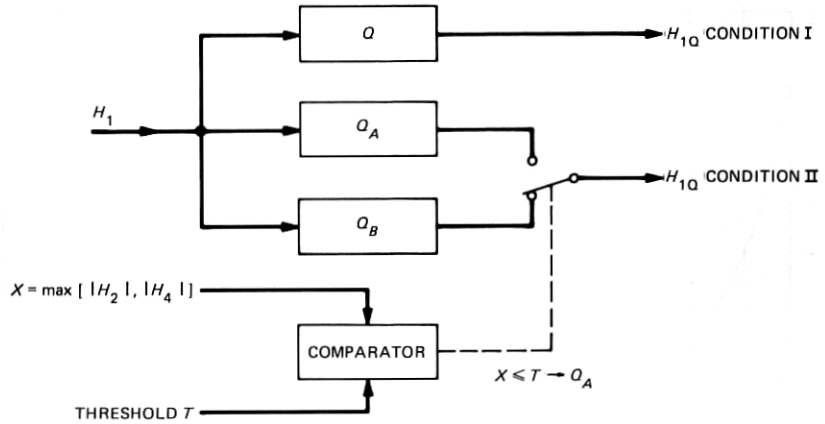

Fig. 7—Experimental setup for quantizer optimization. H_1 is quantized using a PCM quantizer Q and the resulting picture compared with the picture obtained by using PCM quantizers Q_A or Q_B. The choice of Q_A or Q_B depends on whether max $(|H_2|, |H_4|)$ is $<T$ or $\geq T$, respectively.

The results of the test are shown in Table I. Q_A was a quantizer with the same number of levels as the uniform quantizer used for condition I (7 or 6 bits per H_1 sample, as the case may be). Q_B had a smaller number of levels. By changing the threshold T, the percentage of blocks which were coded by Q_A and Q_B were varied. The table gives N_A, the number of coefficients coded by the quantizer Q_A and N_B, the number of coefficients coded by the Q_B. The entropies of the output signals of the quantizers Q_A and Q_B are denoted by E_A and E_B, and the overall entropy is given by E. The entropy of H_1 for condition I with 64-level quantization was 5.66 bits/block, and with 128-level quantization it was 6.64 bits/block.

The table also shows the advantages of adaptation. It is seen that to get the same quality as a picture with 7-bit quantization of H_1, the combination of 7 and 6 bits for Q_A and Q_B, respectively, results in lower entropy than combinations 7 and 5 or 7 and 4 bits. Using the combination of 7 and 6 bits, the saving in entropy is of the order of 15 percent over the nonadaptive quantization.

In order to judge the usefulness of eq. (12), we took values of ℓ_1^*/ℓ_2^* and x_1^* obtained from the above experiments and found that an approximate value of 2 for γ gave a good fit to all the different cases. The precise value of x_1^* which could be obtained from eq. (12c) was checked by evaluating the proportionality constant (between the left-hand side and the right-hand side of the equation) for different cases and was found to vary by about 14 percent. This allows us to conclude that our experimental results are within reasonable agreement of the optimality conditions of eq. (12).

Table I — Results of adaptive PCM quantization of H_1

Test no.	Subject	Bits for quantizer Q_A	Bits for quantizer Q_B	Bits for quantizer Q	Threshold T	Number of blocks in A (average)	Number of blocks in B (average)	Conditional entropy of blocks from Q_A	Conditional entropy of blocks from Q_B	Overall entropy of bits/block
1	I	7	4	7	42	9286	521	6.665	2.922	6.467
	II				47					
2	I	7	5	7	19	6903	2902	6.688	4.230	5.960
	II				23					
3	I	7	6	7	5	2482	7363	6.503	5.518	5.770
	II				5					
4	I	6	4	6	35	8816	990	5.671	3.048	5.340
	II				35					
5	I	6	5	6	12	5729	4066	5.699	4.348	5.140
	II				6					

Entropy of H_1 with 6-bit quantization = 5.657 bits/block
Entropy of H_1 with 7-bit quantization = 6.642 bits/block

3.2 Adaptive DPCM Quantization of H_1

In this section we describe our experiments in adaptive predictive coding of H_1 using a $(2 \times 2 \times 2)$ block. This is done by switching the quantizer in the predictive coder "loop" as a function of a measure of spatial detail. We define the spatial detail S as

$$S = \max [|\overline{H}_4|, \alpha|\overline{H}_2|, \beta|H_4|, \delta|H_2|] \tag{13}$$

This is used as a measure of spatial detail for the transform block consisting of elements $\{\overline{A}, \overline{B}, \overline{C}, \overline{D}, \overline{E}, \overline{F}, \overline{G}, \overline{H}\}$ of Fig. 2. Weight α is used to compensate for the wider separation between the lines due to interlace. We took α to be equal to 1/2. Weight β, which was taken to be 1/2, compensates for the spatial separation between the blocks consisting of $\{A, B, C, D, E, F, G, H\}$ and $\{\overline{A}, \overline{B}, \overline{C}, \overline{D}, \overline{E}, \overline{F}, \overline{G}, \overline{H}\}$. Weight δ was taken to be 1/4 and compensated for the spatial separation as well as effects of interlace.

Using this measure of spatial detail, we performed subjective tests to determine the visibility of noise in $\overline{H}_1$ as a function of S. The visibility function from these tests was used to divide the picture into subpictures. This is done by making a two-step approximation (i.e., piecewise constant approximation with two pieces) to the visibility function. The threshold T, corresponding to the point of separation of the two pieces of approximation, is used to divide the picture. Thus, if $S \leq T$, the block consisting of $\{\overline{A}, \overline{B}, \overline{C}, \overline{D}, \overline{E}, \overline{F}, \overline{G}, \overline{H}\}$ belongs to subpicture I, otherwise it belongs to subpicture II. Each subpicture contains blocks wherein the visibility of a unit of quantization noise is approximately equal.

We performed subjective experiments to determine the characteristics of the quantizer for each subpicture. We used the new predictor for $\overline{H}_1$, as described in Section II. The conditional visibility function, i.e., the visibility function for noise in $\overline{H}_1$ for all blocks belonging to subpicture I, is obtained by adding noise to $\overline{H}_1$ as a function of the unquantized prediction error $(\overline{H}_1 - H_1 - \overline{H}_4 - H_4)$, whenever the spatial detail for the block is less than T. This visibility function is shown in Fig. 8. The quantizer for the prediction error of $\overline{H}_1$ from blocks in subpicture I is obtained by minimizing the mean-square subjective quantization error, using the visibility function as the weighting function. The quantization characteristics for $\overline{H}_1$ of subpicture II are obtained similarly.

We used the quantizers obtained by the above procedure in the real-time system. The picture of Figure 4 was quantized using a 15-level quantizer for subpicture I and a 21-level quantizer for subpicture II. The entropy of the quantized output was 2.41 bits/block for the first transform coefficient. The picture produced by such a quantization was fairly good, although the quantization noise was certainly visible (but not objectionable). The quality of this picture was approximately the same

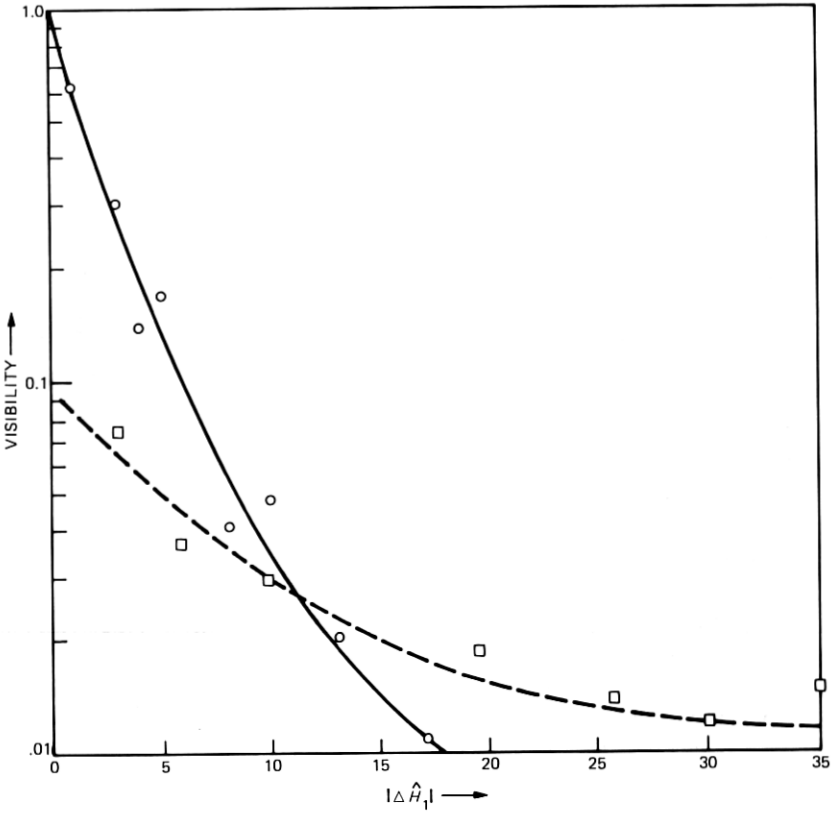

Fig. 8—Conditional visibility functions for noise in H_1. Prediction error $|\Delta \hat{H}_1|$ is used as a control variable. Segment I circles (—) is for the quiet area and segment II (squares) is for the busy area.

as the quality using a nonadaptive 21-level quantizer. Thus the saving in entropy using adaptive quantization was 0.22 bits/block for H_1, which was about 7 percent. We also did adaptive quantization to produce almost perfect picture quality. This required a 17-level quantizer for subpicture I and a 25-level quantizer for subpicture II. The picture quality for this case was equivalent to that produced by 25-level nonadaptive quantization; the advantage of adaptation is about 0.18 bits/block, which amounts to about 6 percent.

IV. SOME COMPARISONS BETWEEN PREDICTIVE CODING AND PREDICTIVE TRANSFORM CODING

In this part, we give a comparison of some of the techniques discussed in our previous paper[1] and the first two parts of this paper. This comparison, done on our real-time system, is limited to the performance in terms of entropy for a given picture quality.

We simulated, for the purpose of comparison, two predictive coding systems in the pel domain. One used the previous element prediction, and the other used a two-dimensional prediction (the predictor for picture element A of Fig. 1 was $B + C - D$). For each of these cases, we optimized the quantizer characteristics by doing subjective experiments in which the visibility of noise was determined by adding noise to the picture element being coded as a function of its prediction error. Pictures of different quality were produced by quantizers having a different number of levels (N). In the case of the previous element predictor, for $N = 23$, a near perfect picture was obtained. There was very slight noise in low-brightness regions. The entropy was 3.57 bits/pel. For $N = 16$, the picture quality obtained was good; however, a slight amount of slope overload and edge busyness was observed. In the low-brightness area the picture was more noisy than for $N = 23$. The entropy was 3.20 bits/pel. For a 13-level quantizer, noise was observed in low-brightness levels. Slope overload and busyness were observed on the edges. The picture was acceptable but impairments were certainly visible. The entropy was 3.02 bits/pel.

Using the two-dimensional predictor and a 16-level optimized quantizer, a near perfect picture was obtained. There was slight slope overload observed in the corner of the mouth of the picture in Fig. 4. The entropy was 3.12 bits/pel. For $N = 13$, a very good picture was obtained except for the slight slope overload in regions of large changes. The entropy in this case was 2.82 bits/pel.

We recall from our earlier work[1] that nonadaptive transform coding (in which the first coefficient is coded using predictive coding techniques with the previous block coefficient as the predictor and the other coefficients are PCM encoded) is capable of generating an excellent picture quality with 2.17 bits/pel. Thus there is almost a 0.95 bit/pel advantage by using transform coding over DPCM with a two-dimensional predictor, and a 1.4 bits/pel advantage over DPCM with a previous element predictor. This advantage is increased by using our new predictor for coding of H_1 and adapting the quantizer. An excellent picture would then be obtained with 1.80 bits/pel. It should be noted, however, that the DPCM techniques which we used for comparison are rather simple, and they can be made more sophisticated to decrease the bit rate significantly.[11] Also, the advantage of transform coding in localizing the transmission error to within a block is lost by doing predictive coding of the coefficients or by adapting the coding using coefficients from many surrounding blocks.

V. SUMMARY AND CONCLUSIONS

We have described techniques for adaptive and predictive coding of Hadamard transform coefficients. We have shown how predictors for

transform coefficients could be designed to reduce the bit rates. For the picture we used, the advantage of using our predictor for H_1 appears to be about 25 percent in terms of entropy reductions over the conventional predictor using the corresponding coefficients from a previous block. We demonstrate this by simulating a predictive coder for coding of H_1. Adaptive quantization, in which a coarse quantizer is used for areas of pictures with larger spatial detail and a fine quantizer is used for relatively flat areas of the picture, was demonstrated by PCM quantization of H_1, as well as by predictive quantization of H_1. We showed that adaptation reduces the bit rate by about 5 to 15 percent without changing the picture quality. We attempted a comparison of the predictive coding in the pel and transform domain. Here, on the basis of picture quality and bit-rate considerations only, we found that using a $2 \times 2 \times 2$ block for transform coding allows a lower bit rate by about 1.8 bits/pel over simple DPCM techniques using the previous element predictor and 1.3 bits/pel over DPCM with a two-dimensional predictor. This comparison does not consider complexity of the encoding schemes. It should be noted that throughout this paper our emphasis has been on investigation of certain techniques rather than a description of a complete coding system; several aspects (e.g., channel errors) which are important to a coding system have not been discussed.

VI. ACKNOWLEDGMENTS

We would like to thank K. Walsh for his help in various phases of this work and the members of the Electronics and Computer Systems Research Laboratory who were test subjects.

REFERENCES

1. F. W. Mounts, A. N. Netravali, and B. Prasada, "Design of Quantizers for Real-Time Hadamard Transform Coding of Pictures," B.S.T.J., *56*, No. 1 (January 1977) pp. 21–48.
2. J. Max, "Quantizing for Minimum Distortion," *IEEE Trans. on Information Theory, IT-6* (March 1960), pp. 7–12.
3. D. O. Reudink, unpublished work, 1971.
4. A. Habibi, "Hybrid Coding of Pictorial Data," *IEEE Trans. on Communications, COM-22*, No. 5 (May 1974), pp. 614–624.
5. M. Ishii, "Picture Bandwidth Compression by DPCM in the Hadamard Transform Domain," *Fujitsu Scientific and Technical Journal*, September 1974, pp. 51–65.
6. J. A. Heller, "A Real Time Hadamard Transform Video Compression System Using Frame-to-Frame Differencing," *NTC-74*, San Diego, 1974.
7. J. A. Roese, A. Habibi, W. K. Pratt, and G. S. Robinson, "Interframe Transform Coding and Predictive Coding Methods," *ICC-75*, San Francisco, 1975.
8. P. A. Wintz, "Transform Picture Coding," *Proc., IEEE* July 1972, pp. 809–820.
9. M. Tasto and P. A. Wintz, "Picture Bandwidth Compression by Adaptive Block Quantization," Technical Report TR-EE-70-14, July 1970, Purdue University, Lafayette, Indiana.
10. J. Gimlett, "Use of Activity Classes in Adaptive Transform Image Coding," *IEEE Trans. on Communications*, July 1975, pp. 785–786.
11. A. N. Netravali and B. Prasada, "Adaptive Quantization of Picture Signals Using Spatial Masking," *Proc. IEEE*, April 1977, pp. 536–548.